Analysis of Structures Containing Sharp Oblique Metal Edges in FDTD Using MAMPs

Chris J. Railton and Dominique L. Paul

***Abstract*—Previous enhancements to the finite difference time domain method have facilitated the analysis of structures such as those containing sharp metal edges which are aligned with the mesh or of smoothly curved metal objects. So far, however, there has been little work on the often encountered situation of thin metal edges which are inclined at an angle to the mesh other than for the special case of diagonal orientation. In this paper, the general case is examined and it is shown that the concept of modified assigned material parameters (MAMPs) can be extended to provide an effective and accurate means of treating this problem. Results are presented for curved microstrip patches, arbitrarily inclined rectangular microstrip patches and for the more complex case of a coplanar fed bow tie slot antenna.**

***Index Terms*—Edges, finite difference time domain (FDTD), modified assigned material parameters (MAMPs), singularities.**

I. Introduction

THE finite difference time domain (FDTD) method has enjoyed ever increasing popularity since its inception in 1966 [1] and throughout its subsequent development from that time until today [2]. It is well known that structures containing sharp metal edges which are aligned to the FDTD mesh can be efficiently analyzed using enhanced FDTD methods. Such enhancements include the use of static field solutions (SFSs), e.g., [3] or modified assigned material parameters (MAMPs), e.g., [4] to account for the singular nature of the field near the edge. In the former case, the FDTD algorithm is expressed as an instance of the method of weighted residuals with singular basis and test functions which take the place of the linear basis functions used in basic FDTD. In the latter case, the effect of the singular behavior of the fields near the edge is accounted for by using an appropriately modified value of permittivity and permeability for the material surrounding the edge. The use of MAMPs has been shown to be simple and effective for a variety of situations including patch antennas [4], lossy coaxial structures [5], wires [6], [7] and microstrip transmission lines [4].

Often, however, a structure will contain sharp edges which are not parallel to each other or are curved. In either case, the edges cannot be aligned with a Cartesian mesh and other ways must be found to perform an analysis. Examples of this include the circular patch antenna described in [8], the inclined microstrip patch described in [9] and [10] and the bow-tie slot antenna described in [11]. Despite the importance of this class of structure, there has been, to the authors' knowledge, little published work in the literature other than for the special, and quite restrictive, case where the edge is diagonal [9], [12]–[14]. In this paper, it is shown that the concept of MAMPs can be extended to provide an effective treatment of general curved and angled metal edges without extra restrictions on the position or shape of the cells. Results using this method are compared to those obtained using basic FDTD with a much finer mesh and also to those obtained using the Dey-Mittra method, [15], which is highly successful for smooth metal boundaries but has limited benefit when used with sharp edges.

Manuscript received August 13, 2009; revised February 25, 2010; accepted March 22, 2010. Date of publication June 14, 2010; date of current version September 03, 2010.

The authors are with the Centre for Communications Research, University of Bristol, Bristol BS8 1BU, U.K. (e-mail: chris.railton@bristol.ac.uk; d.l.paul@bristol.ac.uk).

Color versions of one or more of the figures in this paper are available online at http://ieeexplore.ieee.org.

Digital Object Identifier 10.1109/TAP.2010.2052561

II. General Derivation of MAMPs

The MAMP approach is described in detail in [4] and [5] so only the key features of the method are given here.

Consider Maxwell's equations in integral form

$$\frac{\partial}{\partial t}\iint_S \varepsilon E\cdot dS+\iint_S \sigma E\cdot dS=\oint H\cdot dl \tag{1}$$

$$\frac{\partial}{\partial t}\iint_S \mu H\cdot dS=-\oint E\cdot dl. \tag{2}$$

Applying these to an FDTD mesh in the usual way yields update equations having the following form:

$$\delta y\delta z\left(\frac{\partial}{\partial t}+\frac{\sigma}{\varepsilon}\right)\langle\langle E_x\left(i+0.5,j,k\right)\rangle\rangle_{yz} =\frac{1}{\varepsilon}\begin{pmatrix}\delta y\begin{pmatrix}\langle H_y\left(i+0.5,j,k-0.5\right)\rangle_y\\ -\langle H_y\left(i+0.5,j,k+0.5\right)\rangle_y\end{pmatrix}\\ -\delta z\begin{pmatrix}\langle H_z\left(i+0.5,j-0.5,k\right)\rangle_z\\ -\langle H_z\left(i+0.5,j+0.5,k\right)\rangle_z\end{pmatrix}\end{pmatrix} \tag{3}$$

$$\delta y\delta z\frac{\partial}{\partial t}\langle\langle H_x\left(i,j+0.5,k+0.5\right)\rangle\rangle_{yz} =\frac{1}{\mu}\begin{pmatrix}\delta y\begin{pmatrix}\langle E_y\left(i,j+0.5,k+1\right)\rangle_y\\ -\langle E_y\left(i,j+0.5,k\right)\rangle_y\end{pmatrix}\\ -\delta z\begin{pmatrix}\langle E_z\left(i,j+1,k+0.5\right)\rangle_z\\ -\langle E_z\left(i,j,k+0.5\right)\rangle_z\end{pmatrix}\end{pmatrix} \tag{4}$$

where δx, δy and δz are the cell sizes, i, j and k are the serial numbers of the cell, $\langle a\rangle_x$ is the average of the quantity, a, along an x directed cell edge and $\langle\langle a\rangle\rangle_{xy}$ is the average of the quantity, a, over an xy cell face. The other four update equations can be obtained by rotating the coordinates.

In order to complete this set of equations it is necessary to relate the surface averages on the left hand sides to the line averages on the right hand sides. If the fields are assumed to be constant within each cell then the two are the same and the standard

FDTD update equations are obtained. However, in the vicinity of an edge, since the asymptotic field behavior is known, a more accurate relation can be obtained.

Inspection of the equations shows that the ratios of the surface averages to the line averages can be expressed as a modification to the material parameters in the cell. This leads to a particularly simple and physically meaningful result. For example

$$\left(\frac{\partial}{\partial t}+\frac{\sigma}{\varepsilon}\right)\langle E_x\left(i+0.5,j,k\right)\rangle_x = \frac{1}{\varepsilon\varepsilon_x\delta y\delta z}\begin{pmatrix}\delta y\begin{pmatrix}\langle H_y\left(i+0.5,j,k-0.5\right)\rangle_y\\ -\langle H_y\left(i+0.5,j,k+0.5\right)\rangle_y\end{pmatrix}\\ -\delta z\begin{pmatrix}\langle H_z\left(i+0.5,j-0.5,k\right)\rangle_z\\ -\langle H_z\left(i+0.5,j+0.5,k\right)\rangle_z\end{pmatrix}\end{pmatrix} \tag{5}$$

where

$$\varepsilon_x=\frac{\langle\langle E_x\rangle\rangle_{yz}}{\langle E_x\rangle_x}. \tag{6}$$

As long as the behavior of the x component of the E field is known in the space surrounding the singularity, this parameter is readily calculated. In the final program, only the line integrals are stored, the surface integrals are not explicitly calculated. The update equations for the magnetic field components are dealt with in a similar way giving modified values for the permeability. A major benefit of this formulation is that the metal boundaries can be accounted for simply by changing the value of permittivity and permeability used in the update equations. No extra arithmetic is required after the initial setup.

The presence of a metal boundary will primarily affect the cell containing it but there will also be a lesser effect of neighboring cells. It was found, however, that the accuracy of the results was not noticeably affected if these lesser effects were neglected. Consequently, in the work described here, only the cells which contain a metal boundary are modified.

Modifying the assigned material parameters, particularly if they are reduced, will affect the time step which is required in order to satisfy the CFL stability condition. In this work stability has been obtained by setting the time step to 0.7 of the CFL maximum and also by not allowing any assigned parameters to be less than 0.2.

III. Application to a Curved Patch

Consider the case of a curved metal patch such as the ellipse shown in Fig. 1. For each cell which is cut by the metal edge, the curved boundary is approximated by the sector of a circle. An example of this is given in Fig. 1 for the cell at the center left, position (1,3), of the figure. The approximating circle for this cell is shown in light grey. As part of the pre-processing before the start of the FDTD iterations, the coordinates of all the intercepts between the metal boundaries and the cell edges and cell diagonals are ascertained. Thus, for each cell containing a boundary, there are always three known points which must lie on the approximating circle. For this example, these are labeled

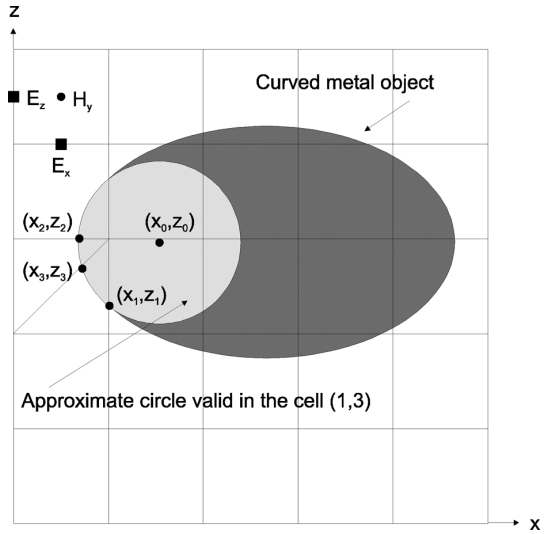

Fig. 1. An elliptical metal object in a coarse FDTD mesh.

as $(\mathrm{x}_1,\mathrm{z}_1)$, $(\mathrm{x}_2,\mathrm{z}_2)$ and $(\mathrm{x}_3,\mathrm{z}_3)$. The center, $(\mathrm{x}_0,\mathrm{z}_0)$, of the circumscribing circle of the triangle formed by these three points can readily be found as follows:

$$x_0=x_1+\frac{y_3'\left(x_2'^2+y_2'^2\right)-y_2'\left(x_3'^2+y_3'^2\right)}{d} \tag{7}$$

$$y_0=y_1+\frac{x_3'\left(x_3'^2+y_3'^2\right)-x_2'\left(x_2'^2+y_2'^2\right)}{d} \tag{8}$$

where

$$\begin{aligned} d&=2\left(x_2'y_3'-x_3'y_2'\right)\\ x_n'&=x_n-x_1\\ y_n'&=y_n-y_1. \end{aligned} \tag{9}$$

The radius of the circle a is given by

$$a=\frac{ABC}{4Area} \tag{10}$$

where

$$\begin{aligned} Area&=\sqrt{k\left(k-A\right)\left(k-B\right)\left(k-C\right)}\\ A&=\sqrt{\left(x_2-x_1\right)^2+\left(z_2-z_1\right)^2}\\ B&=\sqrt{\left(x_3-x_2\right)^2+\left(z_3-z_2\right)^2}\\ C&=\sqrt{\left(x_1-x_3\right)^2+\left(z_1-z_3\right)^2}\\ k&=\frac{A+B+C}{2}. \end{aligned} \tag{11}$$

The electric potential at a point (r,y), caused by a charged conducting circular disk in the x-z plane, centred at the origin and of radius, a, is obtained by solving Laplace's equation in cylindrical coordinates and imposing the condition that the potential is constant on the disk. The result is given in (12)

$$\phi\propto\sin^{-1}\left(\frac{2a}{\sqrt{y^2+\left(r+a\right)^2}+\sqrt{y^2+\left(r-a\right)^2}}\right) \tag{12}$$

where r is the radial distance from the center.

Analytic solutions for the derivatives of the potential with respect to r and y are readily obtained giving the required field distributions

$$E_r(r,y) \propto H_y(r,y) \propto \frac{1}{\sqrt{f_3(r,y)\left(f_3(r,y)-4a^2\right)}} \cdot \left(\frac{r+a}{f_1(r,y)}+\frac{r-a}{f_2(r,y)}\right) \tag{13}$$

$$E_y(r,y) \propto H_r(r,y) \propto \frac{y}{\sqrt{f_3(r,y)\left(f_3(r,y)-4a^2\right)}} \cdot \left(\frac{1}{f_1(r,y)}+\frac{1}{f_2(r,y)}\right) \tag{14}$$

where

$$\begin{aligned} f_1(r,y) &= \sqrt{y^2+(r+a)^2} \\ f_2(r,y) &= \sqrt{y^2+(r-a)^2} \\ f_3(r,y) &= \left(f_1(r,y)+f_2(r,y)\right)^2. \end{aligned} \tag{15}$$

The required integrals can then be calculated numerically.

For example, the modified parameter for the E_x update equation, ε_x, is calculated by first recognizing that for this situation

$$E_x(x,y,z) = E_r\left(\sqrt{(x-x_0)^2+(z-z_0)^2}, y\right)\cos(\theta) \tag{16}$$

where

$$\cos(\theta) = \frac{(x-x_0)}{\sqrt{(x-x_0)^2+(z-z_0)^2}}. \tag{17}$$

Then ε_x is calculated as follows:

$$\varepsilon_x = \frac{\int_{z_n-dz/2}^{z_n+dz/2}\int_{y_n-dy/2}^{y_n+dy/2} E_x(x,y,z)\,dydz}{\int_{x_n}^{x_n+dx} E_x(x,y,z)\,dx} \tag{18}$$

where $(\mathrm{x}_n, \mathrm{y}_n, \mathrm{z}_n)$ are the coordinates of the origin of the cell being updated.

It is noted that although the ellipse is approximated by a series of circles, the calculation of the field distribution around each circle is rigorous and includes the effect of the non-uniform charge distribution. The validity of this approximation is shown by the results presented in the next Section.

IV. Results for an Elliptical Patch

To show that the method works for a curved edge, a series of elliptical patches all having a major radius of 3.6 mm and having minor radii ranging from 0.2 mm – 3.6 mm were placed on a substrate of relative permittivity 2.33 and height 1.12 mm and modelled. Three different FDTD meshes were used in the trials. Firstly, a reference model was run using a very fine mesh having a cubic cell of size 0.08 mm which is $\lambda_0/290$ at 13 GHz. To evaluate the method, results were then obtained using a cell size of 0.56 mm which corresponds to the coarser mesh used in [9]. For comparison, runs were made the Dey Mittra method, [15], as well as the MAMP method which is the subject of this research. Figs. 2 and 3 show the coarse FDTD mesh with the

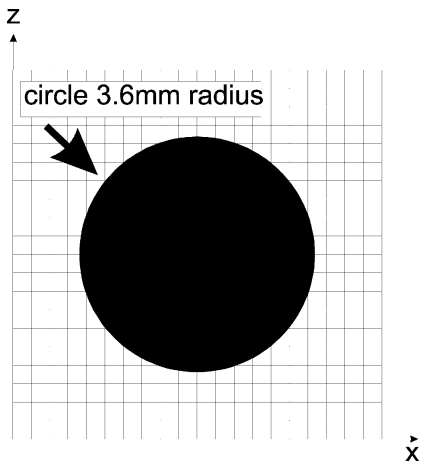

Fig. 2. A circular patch on the coarse (0.56 mm) FDTD mesh.

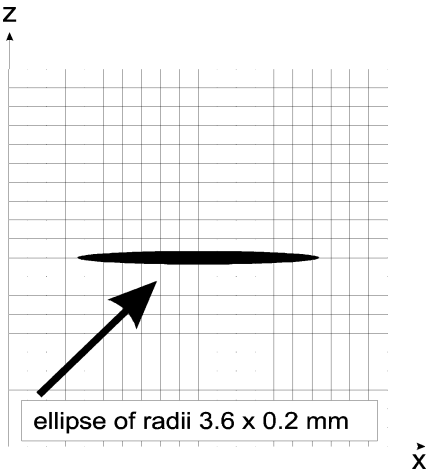

Fig. 3. A thin elliptical patch on the coarse (0.56 mm) FDTD mesh.

circular patch and the sharpest elliptical patch which was analyzed embedded within it.

The resonance frequencies, calculated using the different methods are plotted as functions of the minor radius size in Fig. 4. Here it can be seen that the agreement between MAMPs and the reference is, in almost all cases, significantly closer than between Dey-Mittra and the reference. Despite the minor radius of the sharpest ellipse being less than the FDTD cell size, the accuracy is still improved over other methods.

V. Application to an Inclined Edge

The case of a straight edge which is inclined at an angle to the FDTD mesh, such as the patch shown in Fig. 5, was treated in [10]. The general method is similar to that used for the curved edge except that the appropriate formulae for a straight edge must be used. These are given in (16)–(20) where r is the distance from the edge in the plane of the patch, y is the distance from the edge perpendicular to the plane and w is the width of the patch. These expressions are derived in [16] and are based on the singular behavior of the current distribution on a microstrip line. Unless the width is less than approximately 5 times the cell size, it can be taken as infinite with no significant change in results. Again, each edge is characterized by its intercepts with

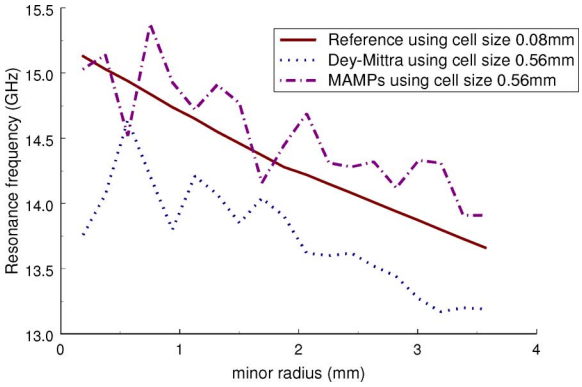

Fig. 4. Resonance frequencies of elliptical patches having a major radius of 3.6 mm and minor radii from 0.2 mm – 3.6 mm.

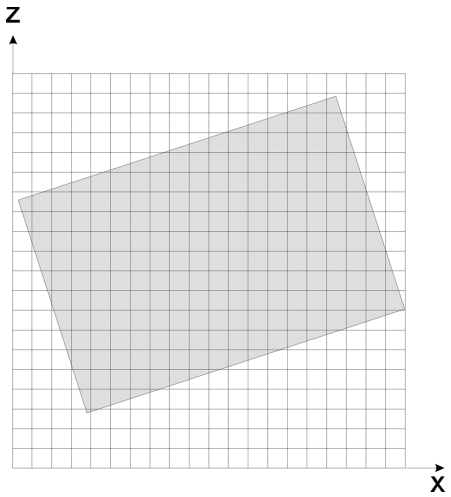

Fig. 5. A patch inclined at 18° to the coarse FDTD mesh.

the cell edges as shown in Fig. 6. To maintain generality in the software implementation, the three intercepts, as used for the curved edge, are always calculated and the choice of field equations is made depending on whether the radius of curvature is greater or less than a chosen threshold value

$$E_r(r,y) \propto H_y(r,y) \propto \mathrm{Im}\left(\sqrt{\frac{w}{(y+ir)^2+\left(\frac{w}{2}\right)^2}}\right) \quad (19)$$

$$H_r(r,y) \propto E_y(r,y) \propto \mathrm{Re}\left(\sqrt{\frac{w}{(y+ir)^2+\left(\frac{w}{2}\right)^2}}\right). \quad (20)$$

In order to apply these expressions to an inclined edge, a change of coordinates is made so that the fields and distances are referred to the FDTD mesh. This is done as follows:

$$E_x(x,y,z) = \sin(\theta)\, E_r\left((z-z_1)\cos(\theta)-(x-x_1)\sin(\theta), y\right) \quad (21)$$

$$E_y(x,y,z) = E_y\left((z-z_1)\cos(\theta)-(x-x_1)\sin(\theta), y\right) \quad (22)$$

$$E_z(x,y,z) = \cos(\theta)\, E_r\left((z-z_1)\cos(\theta)-(x-x_1)\sin(\theta), y\right) \quad (23)$$

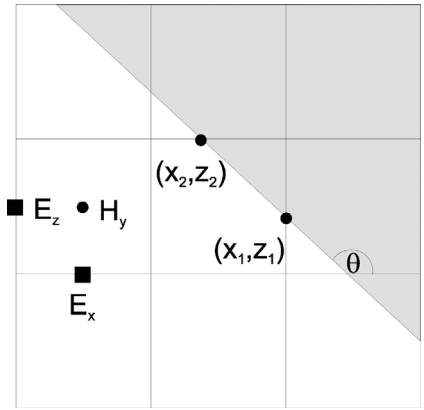

Fig. 6. An inclined edge embedded in the FDTD mesh.

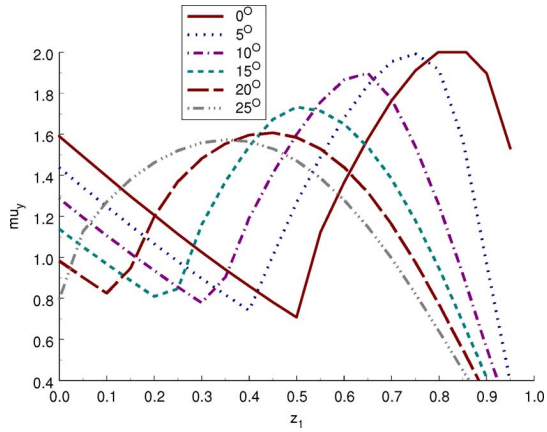

Fig. 7. Values of μ_y versus intercept, z_1, for various values of the angle θ.

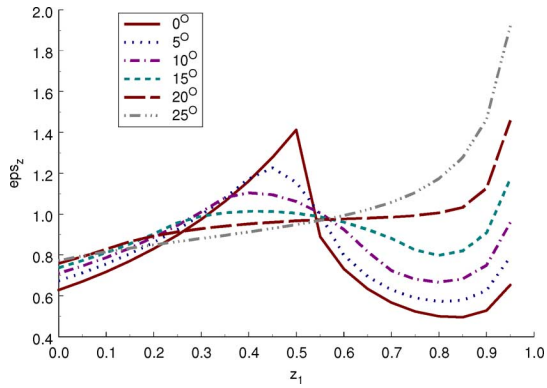

Fig. 8. Values of ε_z versus intercept, z_1, for various values of the angle θ.

and similarly for the H fields.

In order to calculate the modified parameters, using equations such as (6), it is necessary to evaluate the line and surface integrals of the static fields. Where analytical solutions to the integrals are available, such as those given in (24) and (25), these may be used. In the cases where analytical solutions are not available, the integrals may be done numerically. Where numerical integrals are required, they are well behaved and can be readily evaluated using simple algorithms.

In Figs. 7 and 8, examples of the values of the parameters μ_y and ε_z are plotted as functions of the intercept of the edge with

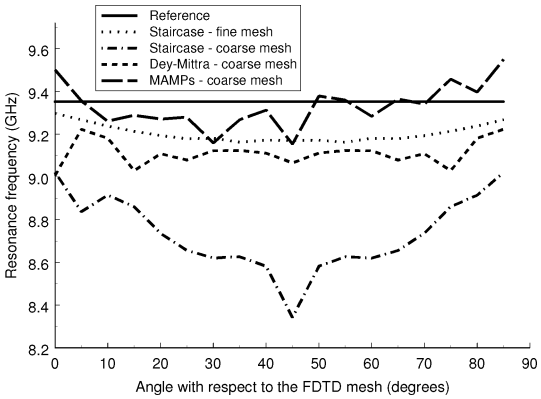

Fig. 9. Calculated resonance frequency for the first mode for different angles or orientation and different methods.

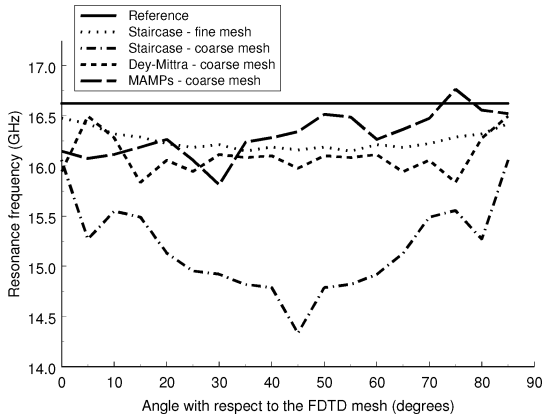

Fig. 10. Calculated resonance frequency for the third mode for different angles or orientation and different methods.

the z axis, z1. Each curve shows the values for a different angle of inclination of the edge with respect to the x axis, θ. It can be seen that, for most cases, the values are in the range 0.4 to 2. In extreme cases where the calculated values are below 0.2, the value of 0.2 is used in order to avoid problems with stability

$$\int H_y dr \propto \int E_y dy \propto \mathrm{Re}\left(\sqrt{w}\ln\left(\frac{\frac{w}{2}}{y+ir+\sqrt{(y+ir)^2+\left(\frac{w}{2}\right)^2}}\right)\right) \tag{24}$$

$$\int E_y dr \propto \int H_y dy \propto \mathrm{Im}\left(\sqrt{w}\ln\left(\frac{\frac{w}{2}}{y+ir+\sqrt{(y+ir)^2+\left(\frac{w}{2}\right)^2}}\right)\right). \tag{25}$$

VI. Results for a Tilted Microstrip Patch

A microstrip patch similar to that used in [9] was considered. This is a patch of size 9.6 mm $\times$ 6.4 mm on a substrate of relative permittivity 2.33 and height 1.12 mm. The same three different FDTD meshes were used in these trials as were used in Section IV. The reference model was run using a very fine mesh having a cubic cell of size 0.08 mm ($\lambda_0/400$) and with the edges aligned with the mesh, i.e., $\theta = 0$. Results were then obtained with the patch orientated at angles of between 0° and 90° and using cell sizes of 0.16 mm and 0.56 mm which correspond to the meshes used in [9].

In Figs. 9 and 10 the predicted values of the first and third resonance frequencies are plotted as a function of the angle of inclination. The horizontal line is from the reference run. It can be seen that the staircase approximation with a 0.16 mm mesh underestimates the frequencies by a small amount whereas the staircase approximation with the coarse, 0.56 mm, mesh gives rise to significant errors of the order of 8%.

In contrast to this, it can be seen that the coarse mesh with modified parameters gives a much reduced average error which is of the order of 1% and is superior to the finer mesh staircase. The approximate saving in computer memory is a factor of 40 and in computer time is a factor of 150. It is noted that the errors obtained using MAMPs are similar to those quoted for the method presented in [9]. However the method of [9] is only applicable to the diagonal case whereas this method is applicable to any angle of inclination.

Calculations were also performed using the Dey-Mittra method [15] which accounts for the position of the edge within the cell but does not account for the singular behavior of the field. It can be seen that although the error is much less than with the staircase approximation it is still, in most cases, substantially greater than with MAMPs.

VII. A Coplanar-Line Fed Bow-Tie Antenna

As a more complex and realistic trial of the technique, a coplanar-fed bow-tie slot antenna of the type investigated in [11] was modeled. This structure, which is shown in Fig. 11, with dimensions given in Table I, presents a number of interesting challenges including the coplanar feed itself which contains a gap of width of only 0.15 mm which is $\lambda_o/200$. In addition there are several inclined sharp metal boundaries and there is the discontinuity between the feed and the antenna itself. In this trial MAMPs were used wherever available to treat the metal edges.

The S_{11} for this antenna was calculated using three different meshes. A coarse mesh having a cell size of (0.5,0.2,0.5) mm, a fine mesh having a cell size of (0.25,0.2,0.25) mm and a very fine mesh having a cell size of (0.125,0.2,0.125) mm. Results using the staircase approximation are shown in Fig. 12. It can be seen that, not surprisingly, the coarse mesh gives a considerable discrepancy when compared with the very fine mesh, particularly for the frequency of the higher resonance. The results from the fine mesh are considerably closer but it can be seen that there is still an appreciable disagreement with very fine mesh which indicates that a still finer mesh is required for full convergence.

Fig. 13 shows the results calculated using the different methods with the coarse mesh compared to the very fine mesh using staircase. The results obtained using the Dey-Mittra approach show a substantial improvement over the staircase approximation but the use of MAMPs gives an even greater improvement. The frequencies of the two resonances predicted by MAMPs with the coarse mesh and staircase with the very

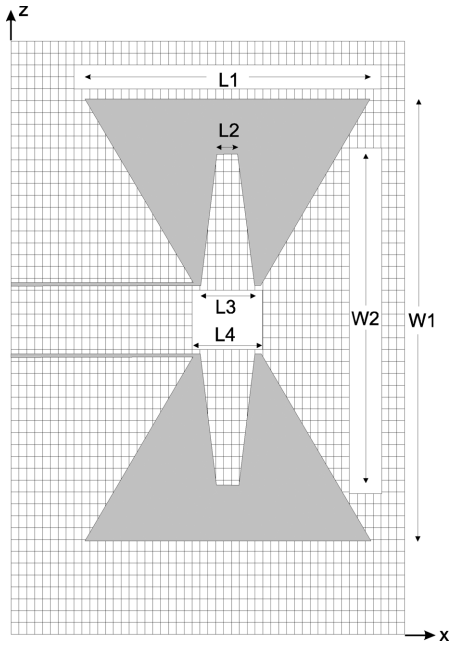

Fig. 11. The plan of a bow-tie slot antenna in the coarse FDTD mesh. The grey area is where there is no metal.

TABLE I
BOW-TIE ANTENNA DIMENSIONS IN mm

W1	19	L4	2.72
W2	14.2	Substrate height	0.762
L1	11.36	Permittivity	3.2
L2	1.76	Feed line width	2.9
L3	2.42	Feed slot width	0.15

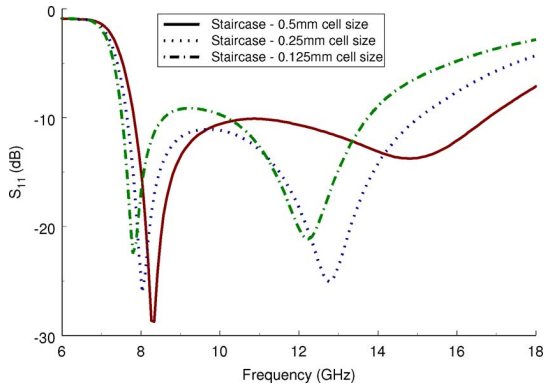

Fig. 12. Calculated S_{11} for the bow-tie antenna using different cell sizes.

fine mesh agree closely although there is still a discrepancy concerning their depth. The required memory and execution time for the former is, however, approximately 16 times less than for the latter.

VIII. CONCLUSIONS

It has been shown that the technique of MAMPs can be extended in order to effectively and efficiently analyze metal patches which are curved or have edges at an arbitrary angle to the FDTD mesh. The technique has proved equally successful

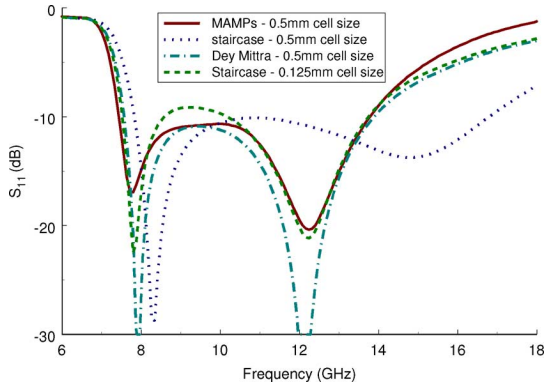

Fig. 13. Calculated S_{11} for the bow-tie antenna using different techniques.

with the challenging situation of a coplanar fed bow tie slot antenna containing several features which are difficult to model using standard FDTD. Unlike previous treatments, the inclination of the edge need not be in the diagonal direction and normally a uniform mesh with a size chosen only for dispersion considerations can be used. This simplifies the mesh generation and also leads to faster and less memory demanding models. It has been demonstrated that a speed up of at around 150 can be achieved compared to a staircase approximation of similar accuracy.

REFERENCES

[1] K. Yee, "Numerical Solution of initial boundary value problems involving Maxwell's equations in isotropic media," *IEEE Trans. Antennas Propag.*, vol. 14, no. 5, pp. 302–307, May 1966.

[2] A. Taflove and S. C. Hagness, *Computational Electrodynamics: The Finite Difference Time Domain Method*, 3rd ed. Boston, MA: Artech House, 2005.

[3] C. J. Railton, B. P. Koh, and I. J. Craddock, "The treatment of thin wires in the FDTD method using a weighted residuals approach," *IEEE Trans. Antennas Propag.*, vol. AP-52, no. 11, pp. 2041–2049, Nov. 2004.

[4] C. J. Railton, D. L. Paul, I. J. Craddock, and G. S. Hilton, "The treatment of geometrically small structures in FDTD by the modification of assigned material parameters," *IEEE Trans. Antennas Propag.*, vol. AP-53, pp. 4129–4136, Dec. 2005.

[5] C. J. Railton, D. L. Paul, and S. Dumanli, "The treatment of thin wire and coaxial structures in lossless and lossy media in FDTD by the modification of assigned material parameters," *IEEE Trans. Electromagn. Compat.*, vol. 48, no. 4, pp. 654–660, Nov. 2006.

[6] T. Noda and S. Yokoyama, "Thin wire representation in finite difference time domain surge simulation," *IEEE Trans. Power Del.*, vol. 17, no. 3, pp. 840–847, Jul. 2002.

[7] Y. Taniguchi, Y. Baba, N. Nagaoka, and A. Ametani, "An improved thin wire representation for FDTD computations," *IEEE Trans. Antennas Propag.*, vol. 56, pp. 3248–3252, Oct. 2008.

[8] C. J. Railton, D. L. Paul, and I. J. Craddock, "Analysis of a 17 element conformal array of stacked circular patch elements using an enhanced FDTD approach," *IEE Proc. Microw. Antennas Propag.*, vol. 150, pp. 153–158, Jun. 2003.

[9] K. P. Esselle and M. Foroughipour, "Analysis of inclined microstrip patch antenna using enhanced FDTD equations," *Electron. Lett.*, vol. 35, no. 11, pp. 853–854, May 1999.

[10] C. J. Railton and D. L. Paul, "Treatment of metal laminas with sharp edges at arbitrary angles to the FDTD grid using MAMPs," in *Proc. Loughborough Antennas and Propagation Conf. (LAPC)*, 2009, pp. 481–484.

[11] A. A. Eldek, A. Z. Elsherbeni, and C. E. Smith, "Characteristics of bow-tie slot antenna with tapered tuning stubs for wideband operation," *Progr. Electromagn. Res. (PIER)*, pp. 53–69, 2004.

[12] K. P. Esselle, M. Okoniewski, and M. A. Stuchly, "Analysis of sharp metal edges at 45 to the FDTD grid," *IEEE Microw. Guided Wave Lett.*, vol. 9, pp. 221–223, Jun. 1999.

[13] F. Lu and B. Chen, "The theory of a singularity-enhanced method for sharp metal edge diagonal to the cell cube in FDTD grid," *IEEE Trans. Antennas Propag.*, vol. 53, no. 3, pp. 1203–1214, Mar. 2005.
[14] S. M. Foroughipour and K. P. Esselle, "The theory of a singularity-enhanced FDTD method for diagonal metal edges," *IEEE Trans. Antennas Propag.*, vol. 51, no. 2, pp. 312–321, Feb. 2003.
[15] S. Dey and R. Mittra, "A locally conformal finite-difference time-domain (FDTD) algorithm for modelling three-dimensional perfectly conducting objects," *IEEE Microw. Guided Wave Lett.*, vol. 7, pp. 273–275, Sep. 1997.
[16] C. J. Railton and J. P. McGeehan, "A rigorous and computationally efficient analysis of microstrip for use as an electro-optic modulator," *IEEE Trans. Microw. Theory Tech.*, vol. 37, no. 7, pp. 1099–1104, Jul. 1989.

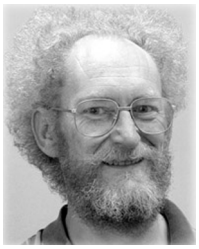

Chris J. Railton received the B.Sc. degree in physics with electronics from the University of London, London, U.K., in 1974 and the Ph.D. degree in electronic engineering from the University of Bath, Bath, U.K., in 1988.

During 1974 to 1984, he worked in the scientific civil service on a number or research and development projects in the areas of communications, signal processing and EMC. Between 1984 and 1987, he worked at the University of Bath on the mathematical modelling of boxed microstrip circuits. He currently works in the Centre for Communications Research at the University of Bristol, Bristol, U.K., where he leads the Computational Electromagnetics group which is engaged in the development of new algorithms for electromagnetic analysis and their application to a wide variety of situations including planar and conformal antennas, microwave and RF heating systems, radar and microwave imaging, EMC, high speed interconnects and the design of photonic components.

Dominique L. Paul received the D.E.A. degree in electronics from Brest University, Brest, France, in June 1986 and the Ph.D. degree from Ecole Nationale Superieure des Telecommunications de Bretagne (LEST-ENSTBr), Brest, in January 1990.

From 1990 to 1994, she was a Research Associate at the Centre for Communications Research, University of Bristol, Bristol, U.K. From 1995 to 1996, she worked as a Research Associate at the Escuela Tecnica Superior de Ingenieros de Telecomunicacion of Madrid, Spain, under a grant from the Spanish Government. Since 1997, she has been a Research Fellow in the Centre for Communications Research, University of Bristol, Bristol, U. K., with a permanent position since 2003. Her research interests include the electromagnetic modelling of passive devices such as microwave heating systems, dielectric structures at millimeter wavelengths, MIMO systems, low profile antennas, conformal antenna arrays and textile antennas for wearable applications.

Dr. Paul is a member of the IET, IEEE Microwave Theory and Techniques Society and IEEE Antennas and Propagation Society.